



Synthesis and Characterization of Al-Doped ZnO Nanoparticles by Electrochemical Method: Photodegradation Kinetics of Methylene Blue Dye and Study of Antibacterial Activities of Al-Doped ZnO Nanoparticles

H. C. Charan Kumar, R. Shilpa and Sannaiah Ananda*

Department of Studies in Chemistry, Manasagangotri, University of Mysore, Mysore-570006, **INDIA**
Email: snananda@yahoo.com

Accepted on 19th December, 2019

ABSTRACT

Al doped ZnO Nanoparticles have been successfully synthesized by electrochemical method which is simple and inexpensive method. The synthesized Nanoparticles were used as a catalyst for the study of photodegradation of methylene blue dye. The electrochemically synthesized Al/ZnO Nanoparticles were characterized by UV-Visible spectroscopy. SEM-EDAX, FT-IR spectrum and X-ray diffraction studies. The study of UV-Visible spectroscopy indicates that the Al/ZnO Nanoparticles shows maximum intensity peak at 230.79 nm in the UV region and there is no absorption peak in the visible region therefore the synthesized Nanoparticles is active under UV light. The band gap energy of synthesized Nanoparticles is 4.64eV it was calculated using Tauc plot. The SEM results show that the synthesized Nanoparticles appear as nanoflakes with agglomerated particles. The EDAX spectra showed that the presence of Al, O and Zn in the synthesized Nanoparticle. The FT-IR spectra reveals that the functional groups present in the molecular structure. The XRD data revealed that the crystal structure of the synthesized Nanoparticles is hexagonal and average crystalline size was found to be 25.51 nm for the Al/ZnO Nanoparticle. The photocatalytic activity of the synthesized Al/ZnO Nanoparticles was examined by the kinetics of photodegradation of methylene blue dye. The degradation efficiency was found to be 96%. The antibacterial activity for ZnO and Al/ZnO Nanoparticles was investigated by using *Bacillus subtilis* MTCC 2763 and *Escherichia coli* MTCC 40 of different bacteria.

Graphical Abstract

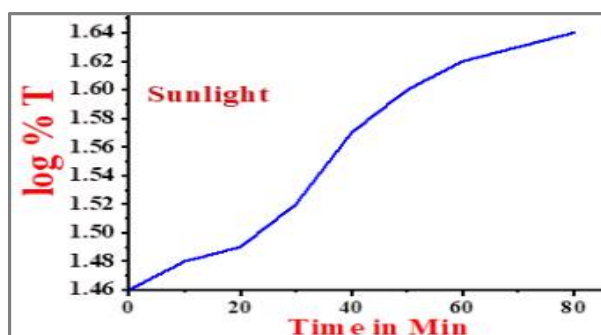


Figure 11. Effect of concentration of Methylene blue dye on the rate of degradation under sunlight.

Keywords: Electrochemical method, Al/ZnO Nanoparticles, Methylene Blue dye, Antibacterial activity.

INTRODUCTION

Zinc oxide is having excellent chemical stability and electrochemical coefficient for a large absorption range as well as very good photo-stability [1, 2]. Zinc oxide is normally introduced and doped with group III elements such as aluminum in order to improve and develop optical transmittance and optical energy band gap by modifying its optical, magnetic electrical and chemical-sensing properties[3-6]. Zinc oxide is recognized as a potential II–VI semiconductor materials having wide band gap (~3.37 eV) and high binding energy (~60 meV) [7-11]. Zinc oxide nanostructures have been extensively examined due to their potential applications in different type of electronic devices [12-15]. Zinc oxide is one of the most interesting materials due to their variety of applications in material science [16, 17]. The Al/ZnO is an n-type doping [18-20]. Al/ZnO Nanoparticles have been prepared by various methods such as hydrothermal method, Co-Participation method, sol-gel method and thermal decomposition etc. Compare to all these methods electrochemical method is best because of less expensive, lower processing temperatures and good control in size and shape of the Nanoparticles. Electrochemical method is a low cost method of manufacturing high quality less agglomerated Nanoparticles [21-28]. Metal doping is one of the most used techniques to these aims[29, 30]. The structural and optical properties of Al/ZnO Nanoparticles could be obviously improved by optimized deposition conditions and controlled doping [31, 32]. In the present paper Al/ZnO Nanoparticles were synthesized by electrochemical method which is an environmentally friendly method by passing an electric current between two or more electrodes separated by electrolyte. The synthesized Al/ZnO Nanoparticles used for photodegradation of methylene blue dye and the kinetics of degradation of methylene blue was studied.

MATERIALS AND METHODS

All chemicals were used to prepare Al/ZnO Nanoparticles were the analytical grades of purity. Al and Zn wire was purchased from Alfa Aesar. Methylene blue dye from lobachemie, Platinum electrode from Elico pvt.ltd. All solution was prepared in double distilled water. The optical properties for prepared Al/ZnO Nanoparticles were studied by uv-visible spectrophotometer (shimadzu-1700 series). The x-ray crystallographic interpretations were performed by x-ray diffractometer (panalytical x-pert) using Cu K α wavelength ($\lambda=1.54$) scanning range from 0 to 70 . The morphological feature for the prepared Al/ZnO study as determined by scanning electron microscopy (SEM-EDEX) from quanta-200 FEI, netherlamds. The elemental analysis for the conformation of prepared Al and Zn is confirmed from energy dispersive X-ray analysis (EDAX). The functional group present in the molecular structure was performed by FT-IR instrument by PerkinElmer spectrum version 10.03.09.

Synthesis of Al/ZnO Nanoparticles by Electrochemical Method: The Al/ZnO Nanoparticle is synthesized by electrochemical method. The experimental process was shown in figure 1. The two electrodes Al and Zn are dipped in the NaHCO₃ solution. The Al and Zn metal electrode is connected to the positive terminal of the battery anode and platinum electrode is connected negative terminal cathode. Using 15 mA current and potential of 10V the experiment was run for 2 hrs with continues stirring. The distance of the anode and cathode during electrolysis was 2 cm. During the electrolysis the Al and Zn electrodes starts to dissolve and give Al ions and Zn ions, which are electrochemically reacted with NaHCO₃ to give Zn(II)oxide/Hydroxide with Al ions. The obtained solid is washed with double distilled water till complete removal of unreacted NaHCO₃. The solid Al/ZnO is centrifuged and calcined for 2 h at 800°C for dehydration and for the removal of hydroxides to get Al/ZnO Nanoparticles. The pH of the dye solution before and after electrolysis was measured and found to be alkaline. Since the mechanism for the synthesized Al/ZnO Nanoparticles is given in scheme 1.

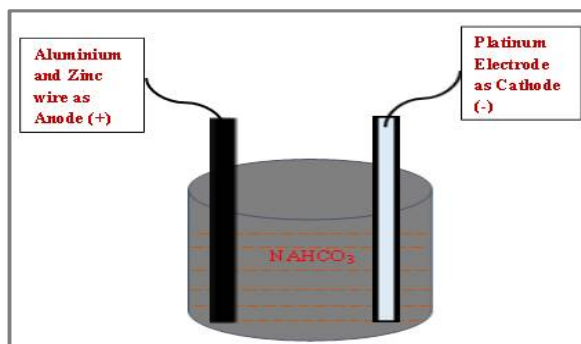
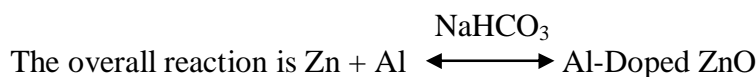
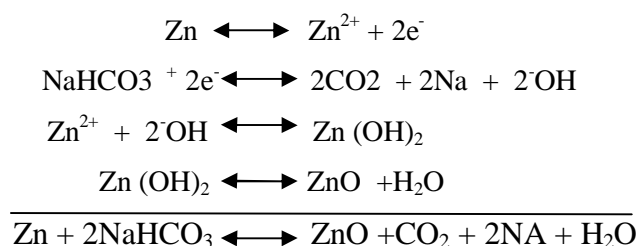


Figure 1. Experimental set up for the electrochemical synthesis of Al/ZnO Nanoparticle



Scheme 1. Synthesized Al/ZnO Nanoparticles.

Determination of Photocatalytic Activities: Methylene blue dye solution (3×10^{-5} M) was prepared by dissolving in distilled water. This solution was used as a test contaminant for evaluating photocatalytic activities of the prepared Al/ZnO Nanoparticles. The exploration was carried out under tungsten-halogen UV-light in order to check the effectiveness of Al/ZnO Nanoparticles. To check the photocatalytic activity, 20 ml of colloidal solution were transferred to centrifuge tube and centrifuged at 800 rpm to remove the dispersed catalyst and the percentage transmittance was recorded for the clear solution. The COD has been reported both before degradation and after degradation of the Methylene blue dye solution using dichromate oxidation method [33, 34]. COD values were calculated by the following equation.

$$\text{COD} = \frac{(\text{Blank-Sample}) \times N_{\text{FAS}}}{V_{\text{Sample}}} \times 8000 \quad \dots(1)$$

RESULTS AND DISCUSSION

UV-Visible Spectra: It is confirmed that from the optical absorption spectra, the absorption band of the Al/ZnO Nanoparticles had been showing a blue shift which is due to particle size in Nano region [35 36]. Figure 2 shows that the synthesized Al/ZnO Nanoparticles has maximum intensity peak at 230.79nm in the UV-region and there is no absorption peak in the visible region, Further, the rate of degradation of dye in presence of sunlight is very slow compare to UV light. The UV-Visible spectrum of Al/ZnO Nanoparticles over the range 200-700 nm showed that the synthesized Nanoparticles are photoactive under ultraviolet radiation. The band gap of synthesized Al/ZnO

Nanoparticles was calculated using Tauc plot [37, 38] by plotting $(\alpha \text{ hm})^{1/2}$ verses $h\nu$. The band gap energy of the synthesized Al/ZnO Nanoparticles was found to be 4.64eV.

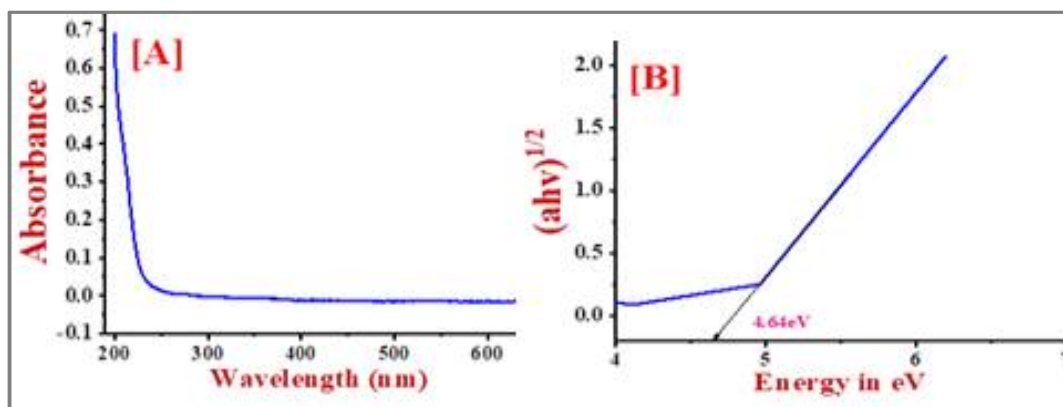


Figure 2. UV-Visible spectra (A) and Tauc plot (B) of Al/ZnO Nanoparticles.

X-Ray Diffraction: The XRD pattern of the synthesized Al/ZnO Nanoparticle samples is shown in figure 3. From the XRD data it is confirm that Al/ZnO Nanoparticles exhibit dominant diffraction peaks appearing at 2 theta is 31.71, 34.16, 36.13, 37.88, 47.54, 56.50, 62.79, 67.91 which are absent in ZnO. The crystal structure of Al/ZnO Nanoparticles belong to hexagonal crystal structure and average crystal size was calculated by using the debye-scherrers equation $D = k\lambda/\beta\cos\theta$ and it was found to be 25.51nm [39]. Where k is an empirical constant equal to 0.9, λ is the wavelength of the X-ray source, β is the full width at half maximum of the diffraction peak and θ is the angular position of the peak. The peak at 31.71° reflects (100) planes, 34.16° reflects (002) planes, 36.13° reflects (101) planes, 37.88° reflects (111) planes and 47.54° reflects (102) planes, 56.50° reflects (110) planes, 62.79° reflects (103) planes, 67.91° reflects (112) planes. There is no much change in the position of the diffraction peaks were observed for ZnO Nanoparticles .Compare to ZnO diffraction peaks the Al/ZnO diffraction peaks show a small shift towards higher θ values. Hence XRD analysis clearly indicates the presence of Al/ZnO Nano composition.

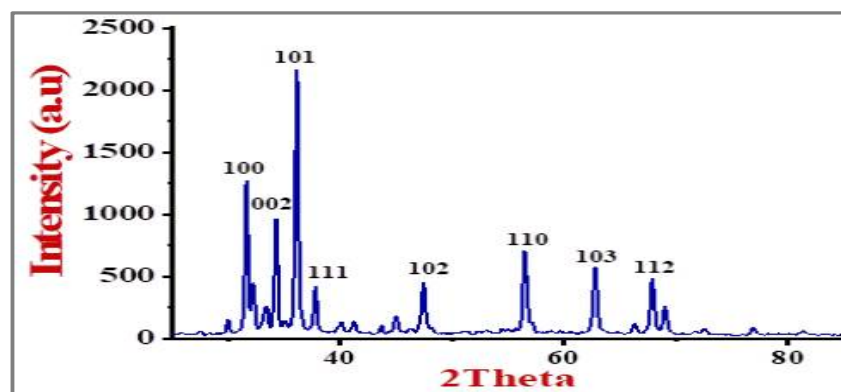


Figure 3. XRD pattern of Al/ZnO Nanoparticles.

Scanning Electron Microscopy (SEM): SEM is High-Resolution microscopy which provides detailed surface data of solid samples. From the figure 5 it is clear that the particles were agglomerated ZnO with Al. The SEM image shows that Al/ZnO nanoparticles are spherical structure and shows nanoflakes, when observed at different magnification. The SEM image shows randomly distributed ZnO with Al grains with smaller size. The EDAX spectrum conformed the presence of Al, Zn and O in the nanomaterial.

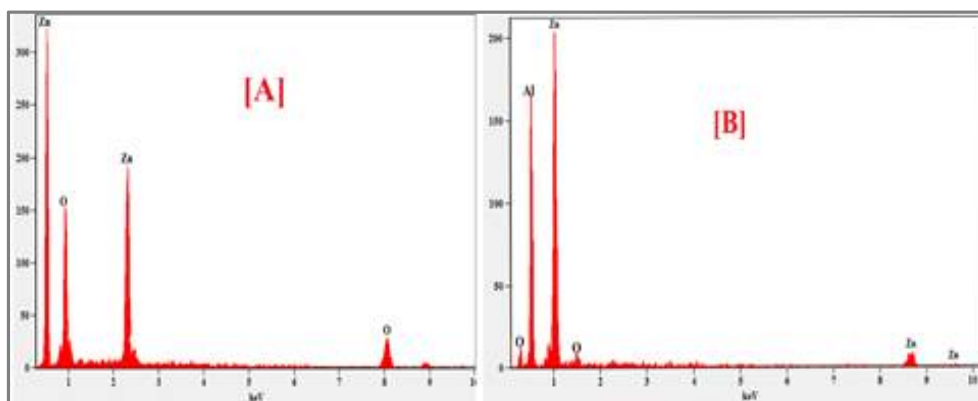


Figure 4. Energy dispersive X-ray analysis spectrum of [A] ZnO and [B] Al/ZnO Nanoparticles.

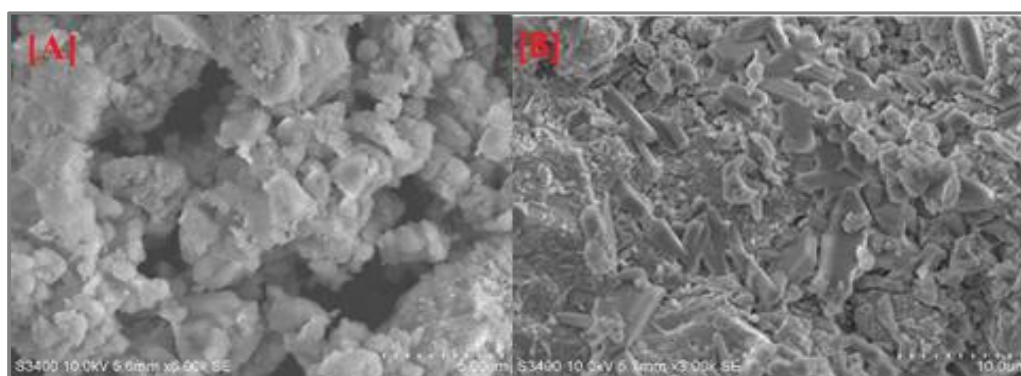


Figure 5. SEM images of electrochemically synthesized [A] ZnO and [B] Al/ZnO Nanoparticles.

FT-IR Spectra: Fourier transform infrared spectroscopy (FT-IR) is an effective technique used to identify the functional groups present in the studied material (Figure 6). The modes of vibration of chemical bonds present in the Al/ZnO nanomaterial were analyzed from the FT-IR spectrum it was recorded in the range 400-4000 cm^{-1} using Perkin Elmer spectrum. The broad peak around 3500 cm^{-1} corresponds to chemically bonded hydroxyl groups. The stretching mode of vibration bands due to C=O observed in 1446 cm^{-1} . The four peaks around 869, 685, 568 and 492 associated with the vibrations of Metal-Oxygen, Aluminium-Oxygen and Metal-Oxygen-Aluminium. So we confirmed that the doped samples show the four peaks around 500-900 cm^{-1} that is agreement to the formation of metal aluminates [1, 6, 20, 42].

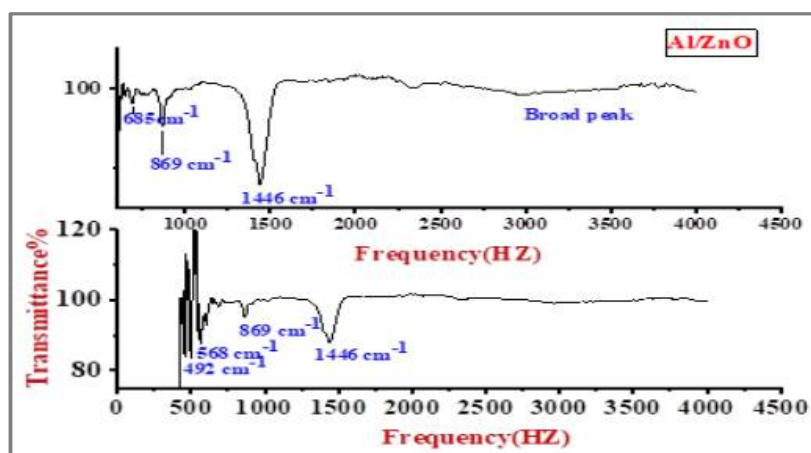


Figure 6. FT-IR spectra for electrochemically synthesized Al/ZnO Nanoparticles.

Photodegradation Kinetics and Cod Measurements

Effect of Concentration of Methylene Blue Dye: The photodegradation process was carried out by taking four different concentration of Methylene Blue dye solution (1×10^{-5} to 4×10^{-5}) with constant weight of Al/ZnO Nanoparticles which is acting as a catalyst. The change in concentration of the methylene blue was reported by change in color by using spectrophotometer. A plot of $\log \%T$ (percentage transmittance of light) versus time was linear up to 60 % of the reaction indicating the disappearance of methylene blue follows first order kinetics (Figure 7). The rate constant values are given in table 1 when increase the methylene blue dye concentration the reaction rate is decreased. The reason beyond that is with increase in the dye concentration, the solution becomes more intense colored and the path length of the photons entering the solution decreases and hence rate is decreased and a few photons reached the catalyst surface. Hence the production of hydroxyl radicals are reduced. Therefore, the Photodegradation efficiency is reduced. The COD values for methylene blue dye solution before and after degradation were measured and are given in table 1. The pH before and after degradation has been reported. It is observed that after degradation the pH of the dye solution is slightly decreased. To account for the mineralization of dye solution COD was examined at different stage. The formation of different radical species during photodegradation was given in scheme 2. The methylene blue dye was found to have mineralized into H_2O , CO_2 and simpler inorganic salts [39]. The Photodegradation efficiency of the photo catalyst was calculated by the following formula,

$$\text{Photodegradation efficiency} = \frac{\text{Initial COD} - \text{Final COD}}{\text{Initial COD}} \quad \dots(2)$$

Table 1. Effect of Photodegradation at different concentration of Methylene blue dye under UV light

10^{-5} [MB]	10^{-4} k Sec ⁻¹	Time taken for 95% Degradation in min	Effect of pH		COD Values in mg L ⁻¹	
			Before degradation	After degradation	Before degradation	After degradation
1.0	3.45	25	10.18	9.20	416	16
2.0	2.64	50	9.80	9.10	592	16
3.0	2.53	90	9.76	8.92	848	32
4.0	1.72	210	9.59	8.76	1040	48

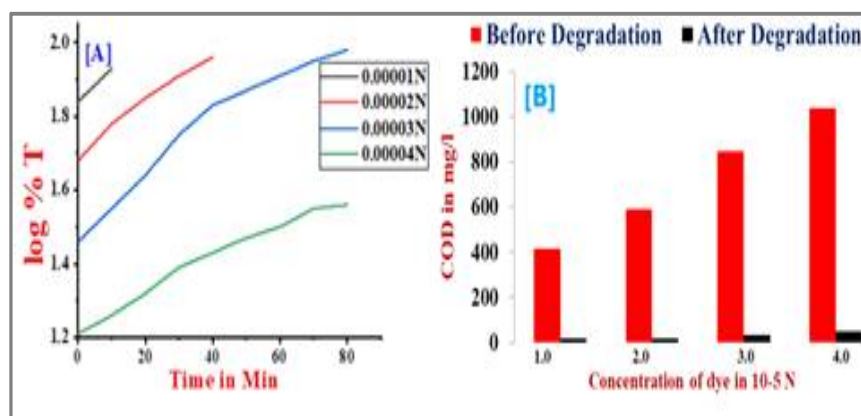
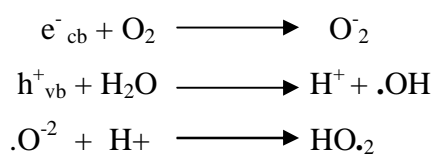
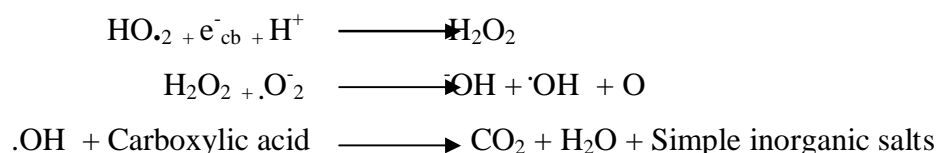


Figure 7[A]. Effect of concentration of Methylene Blue on the rate of degradation and [B] COD values under UV light.





Scheme 2. Formation of different radical species during photodegradation.

Effect of Catalyst Loading: The effect of catalyst was carried out by taking four different amount of catalyst varying from 0.01 to 0.04 g, keeping dye concentration constant in order to study the effect of catalyst loading. The study showed that when increase the catalyst from 0.01 to 0.04 g, the efficiency of methylene blue dye solution was increased. Further, when increase the catalyst above 0.03 g photo activity of the catalyst is decreased, due to aggregation of Al/ZnO Nanoparticles at higher concentration causing a decrease in the number of active sites on catalyst surface and increase in the light scattering of Al/ZnO Nanoparticles at high concentration [40, 41]. This tends to decrease the passage of light through the sample. Further, the present study indicated, from economic point of view, the optimized photocatalyst loading is 0.03g/20 mL⁻¹. The rate constants and COD values are reported in table 2 and Figure 8A and B.

Table 2. Effect of catalyst loading on the photodegradation of Methylene Blue under UV light

Catalyst Al/ZnO in mg	10 ⁻⁴ k Sec ⁻¹	Effect of pH		COD Values in mg L ⁻¹	
		Before degradation	After degradation	Before degradation	After degradation
0.01	0.88	9.87	8.80	848	24
0.02	1.49	9.79	8.88	848	48
0.03	2.53	9.76	8.92	848	32
0.04	1.57	9.72	8.89	848	48

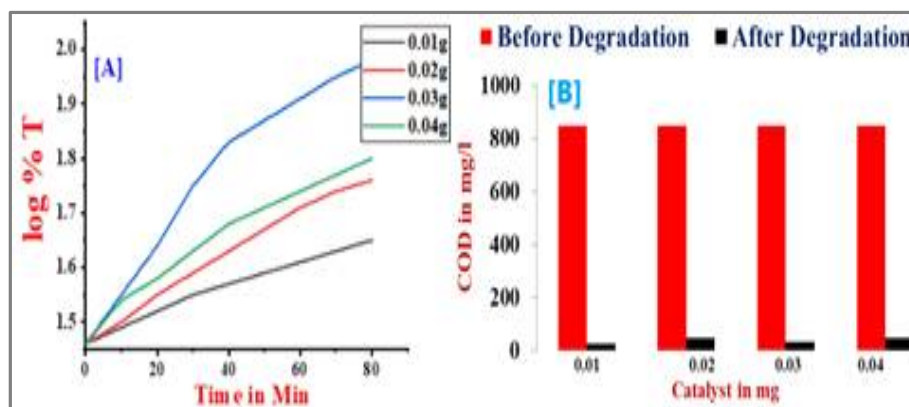
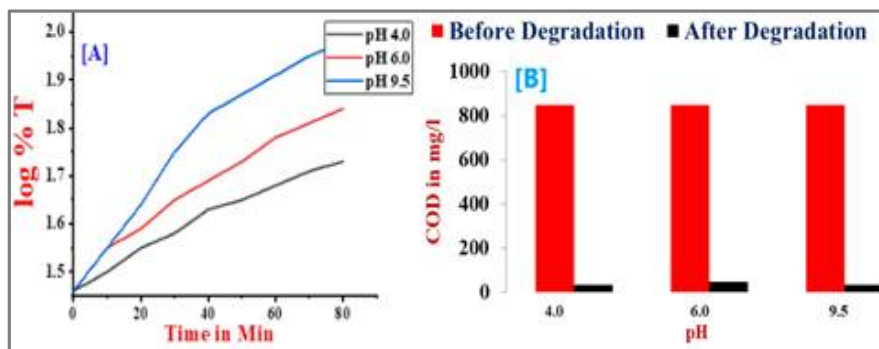


Figure 8. [A] Effect of catalyst loading on the rate of degradation and [B] COD values of dye solution under UV light.

Effect of pH: The pH of the solution is one of the important factors in evaluating the Photodegradation reaction in aqueous medium. In the present work, the pH of the solution was adjusted by adding 0.01 M HCl solution and 0.01 M NaOH. The effect of pH was studied at pH 4.0, pH 6.0 and pH 9.5 by keeping all other experimental conditions constant. From the results it is observed that the rate of photodegradation increases from pH 4.0 to pH 9.5, the degradation rate is increased with increasing pH. Also, the amount of catalyst recovered after the experiment was lowered at lower pH because of the dissolution of the semiconductor oxides at very low pH values. The optimum pH selected is 9.5 at which Photodegradation is high. The rate constant and COD values of pH effect is reported in table 3 and figure 8A and B.

Table 3. Effect of pH on photodegradation of Methylene blue dye under UV light

pH	$10^{-4}k$ Sec ⁻¹	COD Values in mg L ⁻¹		Photodegradation Efficiency %
		Before degradation	After degradation	
4.0	1.30	848	32	96.22
6.0	1.76	848	48	94.33
9.5	2.53	848	32	96.22

**Figure 9** [A]. Effect of pH on the rate of degradation and [B] COD values of dye solution Under UV light.

Effect of Temperature: Temperature is one of the essential factors which effect the rate of photodegradation. To examine the effect of temperature the methylene blue dye solutions were carried out at three different temperatures. From the study it is clear that when temperature is increased the degradation efficiency of dye solution is increased, and observed that the rate of appearance of degradation is not very significant at low temperature. However, the reaction is more significantly influenced at high temperature, since the diffusion rate increased with temperature. An increase of temperature could bring about an increase in the degradation rate [42]. The rate constant and COD values for temperature effect were given in table 4 and figure 10A and B. The thermodynamic parameters were calculated and are reported in table 5.

Table 4. Effect of Temperature on photodegradation of Methylene blue dye under UV light

Temperature in K	$10^{-4}k$ Sec ⁻¹	COD Values in mg L ⁻¹		Photodegradation Efficiency %
		Before degradation	After degradation	
293	1.91	848	24	97.16
298	2.53	848	32	98.22
308	3.76	848	16	98.11

Table 5. Thermodynamic parameters for Methylene blue dye solution

Temperature in K	$\Delta H^\#$ KJ Mol ⁻¹	$\Delta S^\#$ JK ⁻¹ Mol ⁻¹	$\Delta G^\#$ KJ Mol ⁻¹	Ea
293	28.58	-210.07	92.56	7.413
298	28.53	-209.70	93.50	
308	28.45	-210.07	95.72	

Effect of Light Intensity: The photodegradation rate constant is compared with UV light and sunlight. It is perceived that the photodegradation rate constant is increased in UV light compared to sunlight for synthesized Al/ZnO Nanoparticles. The reason beyond that is when a photon interact on a semiconductor (Al/ZnO) the energy overtake the band gap energy of the semiconductor. An electron is jump from the valence band to the conduction band leaving a hole in the valence band

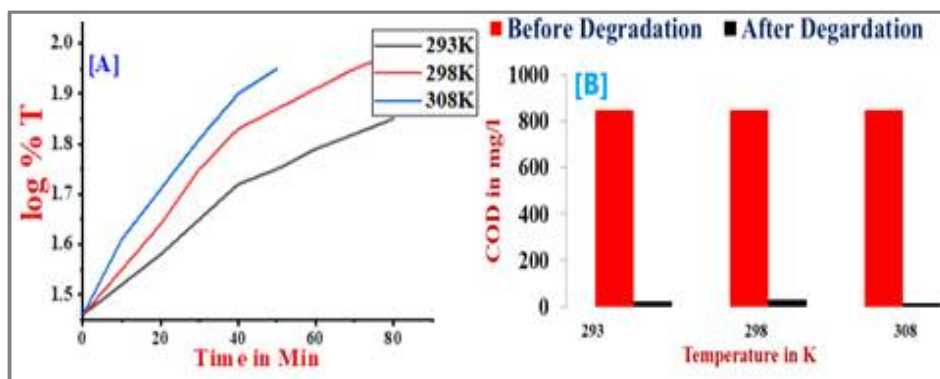


Figure 10 [A]. Effect of Temperature on the rate of degradation and [B] COD values of dye solution under UV light.

The excited state conduction band electrons and valence band hole can recombine and dissipate energy in the form of heat and get trapped into the metastable surface states, respectively with electrons acceptors and donors that happened to be adsorbed on the semiconductor surface. The stored energy is dissipated within a few nanoseconds by recombination in the absence of suitable e^-/h^+ scavengers. If a suitable scavenger is available to trap the electron recombination is prevented i.e. subsequent redox reaction may occur. Therefore, the Al/ZnO Nanoparticles acts as a very good photocatalyst and is active under UV light compared to sunlight. The rate constant for degradation in sunlight is given in table 6 and figure 11. This also supports the observed energy band gap 4.64 eV in the UV visible spectral study.

Degradation in Sunlight: The comparison of photo activity with sunlight was carried out. The photocatalytic experiments were carried out by taking 20 mL of 3.0×10^{-5} N methylene blue dye solution and 0.03 g of synthesized Al/ZnO Nanoparticles in the 50 mL beaker. All experiments were carried out in an open atmosphere between the time of 9.45 A.M to 3 PM in presence of sunlight. It is clear that rate of degradation is very much slow compare to UV light. Hence the synthesized Nanoparticles are active under UV light. The rate constant values are given table 6 and figure 11.

Table 6. Rate of degradation in sunlight

Catalyst 0.03g	Concentration of Methylene Blue dye solution	Sunlight 10^{-4} k S^{-1}	Time taken for 95% Degradation in min	UV light 10^{-4} k S^{-1}	Time taken for 95% Degradation in min
Al/ZnO Nps	3.0×10^{-5}	0.959	270	2.53	90

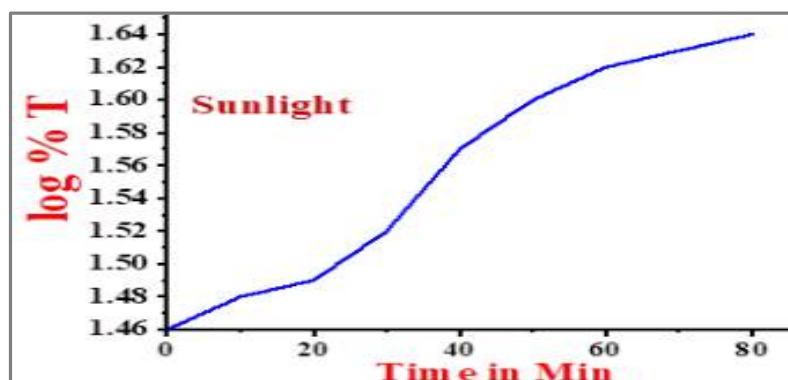


Figure 11. Effect of concentration of Methylene blue dye on the rate of degradation under sunlight.

Reuse of catalyst: The reuse of catalyst was investigated to see the efficiency of photodegradation of the Methylene blue dye solutions. After complete degradation of dye solution, the solution was kept outside for 9 h without exposing the UV light and supernatant liquid sample was decanted. The catalyst was thoroughly washed with double distilled water and reuse for the photodegradation by taking new dye solutions. The reuse of photocatalyst shown almost same degradation efficiency compared to the fresh sample. This can be recommended the photocatalyst can be regenerated and reused.

APPLICATION

Antibacterial Assay: The antibacterial susceptibility of ZnO Nanoparticles and Al/ZnO Nanoparticles was evaluated by using the disc diffusion Kirby-Bauer method in Mueller Hinton Agar Plate [43-45]. The study was subjected to evaluate the ability of these Nanoparticles as antibacterial agent against two bacterial strains was obtained from Microbial Typing Culture Collection (MTCC), Chandigarh, India. Gram-positive *Bacillus subtilis* (MTCC 2763) and gram-negative *Escherichia coli* (MTCC 40) were cultured as per the protocol prescribed by MTCC.

Disc Diffusion Method: Antimicrobial activity was carried out by disc diffusion assay; 20 mL of sterilized and molten Mueller Hinton Agar media was poured in to the sterilized Petri plates. The reference bacterial strains were cultured overnight at 37 °C in Mueller Hinton broth and adjusted to a final density of 10^7 CFU mL⁻¹ by 0.5 McFarland standards. 100 µL of the pathogenic bacteria cultures were transferred onto plate and made culture lawn. The comparative stability of discs containing *Gentamycin* was made. Test ZnO and Al/ZnO Nanoparticles were loaded into 6mm sterile discs and placed on the culture plates and incubated at 37°C for 24 h. The antibacterial activity was evaluated by measuring the diameter of the Zone of inhibition (ZOI) formed around the disc, the antibacterial efficacy of ZnO and Al/ZnO Nanoparticles were determined. All assays were performed in triplicates. The effect of antibacterial activity by ZnO and Al/ZnO Nanoparticles against *Bacillus subtilis* and *Escherichia coli* bacterial strain is as shown in figure12. The results of antibacterial activity of ZnO and Al/ZnONanoparticles are given in table 7. ZnO Nanoparticles were showed good antibacterial activity but less when compare to Al/ZnO Nanoparticles.

The antibacterial susceptibility of ZnO and Al/ZnO Nanoparticle was investigated by zone of inhibition by Kirby-Bauer disc diffusion method. Disposable plates inoculated with the Gram-positive and Gram-negative bacteria, such as *Bacillus subtilis* and *Escherichia coli*.

Table 7. Antibacterial effect of ZnO and Al/ZnO Nanoparticles by Zone of Inhibition (mm) against test strains

Test Bacteria	ZnO Nanoparticles	Al/ZnO Nanoparticles	Positive control Gentamycin (10 µg)
<i>Bacillus subtilis</i> MTCC 2763	13.09 ± 0.01	16.21 ± 0.17	20.35 ± 0.47
<i>Escherichia coli</i> MTCC 40	15.91 ± 0.09	18.82 ± 0.04	21.03 ± 0.43

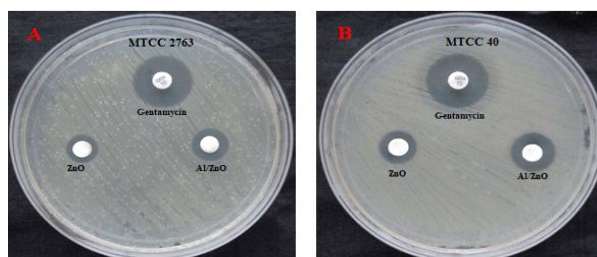


Figure 12. Appearances of inhibitory zones with (A) Gram-positive *Bacillus subtilis* (MTCC 2763) and (B) gram-negative *Escherichia coli* (MTCC 40).

CONCLUSION

In the present study, the Al/ZnO Nanoparticles were synthesized by electrochemical method. The photodegradation by this semiconductor offers a green technology for removal of organic dyes present in waste water and industrial effluents. The photocatalytic study for the synthesized Al/ZnO Nanoparticles was investigated by the kinetics of photodegradation of Methylene blue dye by using UV light. Kinetics of photodegradation of Methylene blue dye recommended that the dematerialize of dye follows 1st order kinetics. The photodegradation rate is low in sunlight when compare to UV light, hence the synthesized Al/ZnO Nanoparticles acts as a very good photocatalyst and is active under UV light. The complete degradation of dye solution was confirmed by COD measurement. The COD values revealed that 96% of the dye had been degraded. The synthesized Nanoparticles show appreciably good inactivation of different strains of bacteria.

ACKNOWLEDGEMENT

Charan Kumar H.C is grateful to UGC-BSR Programme for the award of a project fellow and thanks the IOE, UPE, CPEPA, DST-PURSE and university of Mysore.

REFERENCES

- [1]. V. T. Bhugul, G. N. Choudhari, Synthesis and Studies on Nanocomposites of polypyrrole- Al-doped zinc oxide Nanoparticles, *International Journal of Scientific and Research Publications*, 2015, 5(1), 1-5.
- [2]. Y. He, A novel emulsion route to sub- micrometer polyaniline/nano- ZnO composite fiber' *Applied surface science*, **2010**, 249, 7-18.
- [3]. Affa Rozana Abd Rashid, NurAthirahMohdTaib, Tuan NurHazwani, Wan Maisarah Mukhtar, Influence of Annealing Temperature on Optical Properties of Al Doped ZnO Nanoparticles via Sol-gel Methods, Published by AIP Publishing. 978-0-7354-1679-6
- [4]. S. M. Al-Hilli, R. T. Al-Mofarji, and M. Willander, *Appl. Phys. Lett.*, **2006**, 89, 1731191–1731193.
- [5]. B. Chatpong, C. Krisana, P. Wisanu, T. Wicharn, SainsMalaysiana, **2013**, 42(2), 239-246.
- [6]. V. reeram , M. Sivanath, K.S atyanarayana ,Studies on Structural And Optical Properties of Al Doped Zno Nanopowders, *International Journal of Engineering Science Invention*, 38-45.
- [7]. G. VijayaPrakash, R. Singh, A. Kumar, R.K. Mishra, *Mater. Lett.*, 2006,60, 1744–1747.
- [8]. Sethuraman Gayathri, Oriparambil Sivaraman, Nirmal Ghosh, S. Sathish kumar, P. Sudhakara, J. Jayaramudu, S. S. Ray, Annamraju Kasi Viswanath, Investigation of physicochemical properties of Ag doped ZnO nanoparticles prepared by chemical route, *Appl. Sci. Lett.*, **2015**, 1(1), 8-13.
- [9]. G. Vijaya Prakash, K. Pradeesh, Ashwani Kumar, Rajesh Kumar, S. Venugopal Rao, M. L. Markham, J. J. Baumberg, Fabrication and optoelectronic characterisation of ZnO photonic structures, *Materials Letters*, **2008**, 62, 1183–1186.
- [10]. E. Chalangar, Influence of morphology on electrical and optical properties of graphene/Al-doped ZnO-nanorodcomposites, *Nanotechnology*, 2018, 29, 415201.
- [11]. A. Panwar, N. K. Pandey, S. K. Misra, Doped and Undoped Zinc Oxide as Humidity Sensor, *International Journal o Engineering Sciences and Research Technology*, 7(1), 179-185.
- [12]. M. C. Shin, G. T. Lay, H. L. Wei, H. S. Yen, H. H. Min, ZnO, Al thin film gas sensor for detection of ethanol vapor, *Sensors*, **2006**, 6, 1420–1427,.
- [13]. V. R. Shinde, T. P. Gujar, C. D. Lokhande, Enhanced response of porous ZnO nanobeads towards LPG: Effect of Pd sensitization, *Sens. Actuators B Chem.*, **2007**, 123, 701–706.
- [14]. O. Wurzinger, G. Reinhardt, CO-Sensing Properties of Doped SnO₂ Sensors in H₂-Rich Gases, *Sensors and Actuators B*, **2004**, 103(1-2), 104-110.
- [15]. Parameters optimization for synthesis of Al-doped ZnO nanoparticles by laser ablation in water Nikša Krstulovic, Krešimir Salamon, Ivana Capan. *Applied Surface Science* 440 (2018) 916–925

- [16]. U. Ozgur, Ya.I. Alivov, C. Liu, A. Teke, M.A. Reshchikov, S. Dogan, V. Avrutin, S.J. Cho, H. Morkoc, A comprehensive review of ZnO materials and devices, *J. Appl.phy.*98(2005) 041301-42100
- [17]. P. M. Aneesh, M. R. Shijeesh, Arun Aravind, M. K. Jayaraj, Highly luminescent undoped and Mn-doped ZnS nanoparticles by liquid phase pulsed laser ablation, *Appl. Phys.* 2014, A 116, 1085–1089.
- [18]. Anne Aimable, Tomasz Strachowski, Ewelina Wolska, Witold Lojkowski, Paul Bowen., Comparison of two innovative precipitation systems for ZnO and Al-doped ZnO nanoparticle synthesis Processing and Application of Ceramics, **2010**, 4 (3), 107–114
- [19]. S. Guillemet-Fritsch, M. Aoun-Habbache, J. Sarrias, A. Rousset, N. Jongen, M. Donnet, P. Bowen, J. Lemaitre, High-quality nickel manganese oxalate powders synthesized in a new segmented flow tubular reactor, *Solid State Ionics*, **2004**, 171, 135–140.
- [20]. Ramesh Babu et al Studies on the Structural, Optical and Magnetic Properties of Al doped ZnO Nanoparticles, *R.Int.J. ChemTech Res.* **2014-2015**, 7(3), 1206-1211.
- [21]. Thomas Straube, Jürgen Linder, Christian B. Mayer, Thomas Mayer-Gall, Torsten Textor, Jochen S. Gutmann, Polyol synthesized aluminum doped zinc oxide nanoparticles-influence of the hydration ratio on crystal growth, dopant incorporation and electrical properties a, *Materials Today, Proceedings*, **2017**, 4, S253–S262
- [22]. J. Puetz, Al, N Dahoudi, M. A. Aegerter, Processing of Transparent Conducting Coatings Made With Redispersible Crystalline Nanoparticles, *Advanced Engineering Materials*, **2004**, 6(9), 733–737.
- [23]. H. Liu, V. Avrutin, N. Izyumskaya, Ü. Özgür, H. Morkoç, Transparent conducting oxides for electrode applications in light emitting and absorbing devices, *Superlattices and Microstructures*, **2010**, 48(5), 458-484.
- [24]. S. R. Brintha, M. Ajitha, Synthesis, Structural and Antibacterial Activity of Aluminium and Nickel Doped ZnO Nanoparticles by Sol-gel Method, *Asian Journal of Chemical Sciences* **2016**, 1(1), 1-9.
- [25]. R. Wahab, S. G. Ansari, Y. S. Kim, M. A. Dar, H. S. Shin. Synthesis and characterization of hydrozincate and its conversion into zinc oxide nanoparticles, *J. Alloys and Comp.*
- [26]. Satyanarayana Talam, Srinivasa Rao Karumuri, Nagarjuna Gunnam, Synthesis, characterization and spectroscopic properties of Zn nanoparticles, *ISRN Nanotechnology*, **2012**, Article ID 372505.
- [27]. Morteza Shakeri Shamsi, Mehdi Ahmadi, Mohammad Sabet, Al Doped ZnO Thin Films; Preparation and Characterization, *J. Nanostruct.*, **2018**, 8(4), 404-407.
- [28]. Leonardo Palmisano Faten Ajala, Abdesslem Hamrouni, Ammar Houas, Hinda Lachheb, Bartolomeo Megna, Francesco Parrino. The influence of Al doping on the photocatalytic activity of nanostructured ZnO: The role of adsorbed water, *Applied Surface Science*, **2018**, 445, 376–382
- [29]. M. Bellardita, H. A. El Nazer, V. Loddo, F. Parrino, A. M. Venezia, L. Palmisano, Photoactivity under visible light of metal loaded TiO₂ catalysts prepared by low frequency ultrasound treatment, *Catal. Today*, **2017**, 284, 92–99.
- [30]. P. Gowrisankar V. Balaprakash, R Rajkumar, S Sudha, Preparation and characterization of aluminum doped zinc oxide (AZO) nanorods, *Indian Academy of Sciences*, **2018**, 43(86).
- [31]. D. Cossement, J. M. Streydio Fabrication of ZnO polycrystalline layers by chemical spray, *J. Cryst. Growth*, **1985**, 72 (1–2), 57–60
- [32]. Priyanka Jood, Rutvik J. Mehta, Yanliang Zhang, Germanas Peleckis, Xiaolin Wang, Richard W. Siegel, Theo Borca-Tasciuc, Shi Xue Dou, Ganpati Ramanath, Al-Doped Zinc Oxide Nanocomposites with Enhanced Thermoelectric Properties, *NanoLett.* **2011**, 11, 4337–4342
- [33]. G. Chaitanya Lakshmi, S. Ananda, C. Somashekar, Ranganathaiah, Synthesis of ZnO/ZrO₂ nanocomposites by electrochemical method and photocatalytic degradation of Fast green dye, paper dyeing and printing press effluent, *Int J Adv Mater Sci.*, **2012**, 3, 221-237.

- [34]. K. Byrappa, A. K. Subramani, S. Ananda, K. M. L. Rai, R. Dinesh, M. Yoshimura. Photocatalytic degradation of rhodamine B dye using hydrothermally synthesized ZnO, *Bull Mater Sci.*, **2006**, 29,1-6
- [35]. SubhashKondawar, RituMahore, Ajay Dahegaonkar, ShikhaAgrawal Electrical Conductivity of Cadmium Oxide Nanoparticles Embedded Polyaniline Nanocomposites, *Advances in Applied Science Research*, **2011**, 2 (4):401-406
- [36]. Ma, X. Y., Lu, G. X., Yang, B. J., *Applied Surface Science*, 2002, 187, 235-238.
- [37]. T. P. Sharma, D. Patidar, N. S. Saxena, K. Sharma, *Indian Journal of Pure and Applied Physics*, **2006**, 44, 520–615
- [38]. B. cullity, Elements of X-ray diffraction, A.W.R.C inc, massachusetts, **1967**.
- [39]. K. R. Raksha, Sannaiah Ananda, An investigation on kinetics of photocatalysis, electrical property and biological activity of electrochemically synthesized ZnS and Ru: ZnS nano photocatalysts, *J. Applicable Chem.*, 2014, 3(1), 397-412.
- [40]. B. Kraeutler, A.J. Bard, Heterogeneous Photocatalytic Decomposition of Saturated Carboxylic Acids on TiO₂ Powder. Decarboxylative Route to Alkanes, *J. Am. Chem. Soc.*, **1978**, 100, 5985–5992
- [41]. H. C. Charan Kumar, R. Shilpa, V. Ravi Shankar Rai, Sannaiah Ananda, Synthesis and Characterization of NiO Nanoparticles by Electrochemical Method: Photodegradation Kinetics of Indigo Carmine Dye and Study of Antibacterial Activities of NiO Nanoparticles, *J. Applicable Chem.*, **2019**, 8(2), 622-633
- [42]. L . Wei, C. Shifu, Z. Wei, Z. Sujuan, Titanium dioxide mediated photocatalytic degradation of methamidophos in aqueous phase. *Journal of Hazardous materials*, **2009**, 164, 154160.
- [43]. A. W. Bauer, W. M. M. Kirby, J. C. Sherris, M. Turck, Antibiotic susceptibility testing by a standardized single disk method, *American journal of clinical pathology*, **1966**, 45(4), 493-496.
- [44]. Khawlah Salah Khashan, Ghassan Mohammad Sulaiman , Farah Abdul Kareem Abdul Ameerland Giuliana Napolitano Pak.Synthesis, characterization and antibacterial activity of colloidal NiO nanoparticles, *J. Pharm. Sci.*, **2016**, 29(2), 541-546.
- [45]. R. S. Raveendra, P. A. Prashanth, S. Sathyarayani, B. M. Nagabhushana, Nio Nanoparticlesand Its Antibacterial activity, *International Journal of Scientific Research and Review*, **2018**, 7(9).